Advances in Engineering Research : Possibilities and Challenges
ISSN Print: 3079-5192
ISSN Online: 3079-5206
https://doi.org/10.63313/AERpc.9022

Research on the Amplitude-Frequency Characteristics of the Lateral Vibration of the BTA Deep Hole Machining System

Kun Li
School of Mechanical and Power Engineering, Henan Polytechnic University, Jiaozuo 454003, China
Email: 18339170117@163.com

How to cite this paper: Li, K. (2025). Research on the Amplitude-Frequency Characteristics of the Lateral Vibration of the BTA Deep Hole Machining System. Advances in Engineering Research : Possibilities and Challenges, 1(2), 77–89. ISSN Print: 3079-5192, ISSN Online: 3079-5206.
https://doi.org/10.63313/AERpc.9022
Published: 2025-05-12

Abstract

The lateral vibration of the boring bar in the precision BTA deep-hole boring pro-cess cannot be ignored. This chapter mainly studies a type of vibration situation in which the boring bar has lateral vibration caused by the elastic bending defor-mation of the tool when the tool system rotates and cuts into the workpiece during the boring process. Analyze the BTA deep-hole boring machining system, use the multiple scale method to obtain the amplitude-frequency response equation of the vibration model; use numerical simulation techniques to obtain phase diagrams and amplitude-frequency diagrams to analyze the amplitude-frequency character-istics, and obtain the dynamic behavior of the BTA deep-hole boring system con-sidering the elastic deformation of the tool under the influence of fluid with the change of various parameters, revealing the evolution mechanism of the nonlinear dynamic behavior of the BTA deep-hole machining system with the change of process parameters.

Keywords

BTA deep hole machining; Transverse vibration; Amplitude-frequency response; Amplitude-frequency characteristics

1. Introduction

The vibration generated by the BTA drill rod during deep hole machining significantly affects the surface quality of the workpiece. Unstable vibration can create irregular wave pat-terns on the workpiece surface, increase surface roughness, degrade workpiece performance, and in severe cases, impair its functionality. This paper mainly studies a kind of vibration situation in which the drill pipe vibrates due to the elastic bending deformation of the cutting tool when the drill pipe cutting tool system rotates and cuts into the work piece. Lie Li, Yuchen Ren[1] and others developed a nonlinear model to study the vibration stability in the boring process and the influence of damping and stiffness related nonlinear parameters on the vibration characteristics of the boring bar. Ren, Yong sheng [2] conducted a nonlinear dynamic analysis on the cutting process of composite tools. They established the chatter equation of the cut-ting system by taking into account the high-order bending deformation of the cutting tools. Ma Bole, Ren Yong sheng[3] conducted a nonlinear dynamic analysis on the cutting process of the inextensible composite boring bar, derived the nonlinear motion equations of the system, and approximately solved the steady-state forced response of the cutting system under the periodically changing cutting force by using the multi-scale method. Du Xiao kang, Zhang Jing[4] introduced an improved modeling method for the dynamic analysis of a rotating cantilever beam with a free-end mass. They introduced the balanced axial deformation into the axial motions and derived the free vibration analysis equations for the rotating cantilever beam with a free-end mass. For the research on dynamic cutting, Du Weitao[5] put forward a new dynamic cut-ting force prediction model for the boring process analysis to take into account the time changing tool path and chip breakage during the machining process. Andrew Longstaff[6] studied the dynamic interaction between the cutting tool and the workpiece during the cutting process and its influence on cutting stability. Chun jin Zhang, Xi Chen [7-9] and others studied the influence of the cutting tool vibration on the cutting force during the cutting process in order to reflect the impact of the cutting tool vibration in the machining process. In the deep hole machining system, taking into account the influence of cutting fluid, Al-Wedyan H M, Weinert K et al.[10-12] studied the whirling problem of the BTA deep hole boring bar, established the whirling equation of the deep hole boring bar, explored the conditions for the generation of the boring bar's whirling, and laid a certain foundation for studying the stability of the boring bar system. They also studied the lateral vibration problem of the free drill pipe under the action of fluid-structure coupling and obtained the parametric conditions for judging bifurcation. Zhao Wu[13-15] and others analyzed the influence of different system parameters and fluid parameters on the changes in the nonlinear dynamic behavior of the system.

Through the simulations of characteristics, the evolution mechanism of the nonlinear dynamic behavior of the BTA deep hole machining system when parameters change is revealed, and the chaotic parameter intervals of the lateral vibration of the system are analyzed. This research can provide theoretical guidance for engineering applications.

2. Analysis of the amplitude-frequency characteristics of the BTA deep hole machining system

2.1. Solution of amplitude-frequency response

The BTA deep hole machining system is complicated and comprises a full-length machining layout schematic, as illustrated in Fig.1. The stability of the drilling rod has a direct impact on the quality and efficiency of the workpiece machining process.

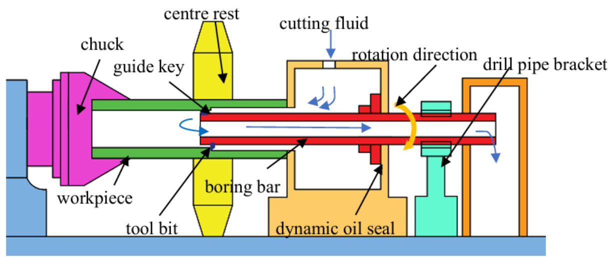

Figure 1. Schematic layout of the whole system of BTA deep hole m-achining system for full-length machining.

The schematic diagram of the BTA deep hole machining drill bar-tool system, as illustrated in Fig.1, are employed to analyse the force exerted on the tool during the dynamic cutting process. This analysis aims to elucidate the mechanism through which the tool influences the transverse vibration of the drill bar generated during the dynamic cutting process, as well as its impact on the stability of the system . Explore the influences of the fluctuations of stiffness coefficient, damping coefficient and force amplitude coefficient on the main resonance of the lateral motion of boring bars. The multi-scale method is used to solve the model, and the basic perturbation method is employed to obtain the formal solution.

$$x(t) = x_0(t) + \varepsilon x_1(t) + \varepsilon^2 x_2(t) + \cdots \tag{1}$$

In the expansion, secular terms (secular terms in perpetuity) which are formed by multiplying sine and cosine functions with t，εt，ε²t，... will appear, making the solution form non-uniformly valid. The multi-scale method makes use of selecting different time variable parameters. Based on this principle, new independent independent variables are introduced.

$$T_n = \varepsilon^n t \qquad \text{n=0,1,2,}\cdots \tag{2}$$

The derivative with respect to t can be expressed by the partial derivative with respect to Tn.

$$\begin{cases} \dfrac{d}{dt} = \dfrac{\partial}{\partial T_0}\dfrac{\partial T_0}{\partial t} + \dfrac{\partial}{\partial T_1}\dfrac{\partial T_1}{\partial t} + \dfrac{\partial}{\partial T_2}\dfrac{\partial T_2}{\partial t} + \cdots = D_0 + \varepsilon D_1 + \varepsilon^2 D_2 + \cdots \\ \dfrac{d^2}{dt^2} = (D_0 + \varepsilon D_1 + \varepsilon^2 D_2 + \cdots)^2 = D_0^2 + 2\varepsilon D_0 D_1 + \varepsilon^2 (D_1^2 + 2D_0 D_2) + \cdots \end{cases} \tag{3}$$

Where $D_i = \partial / \partial T_i \quad i = 0,\ 1,\ 2\cdots$, Let the solution of the differential equation be:

$$x(t) = x_0(T_0, T_1, T_2, \cdots) + \varepsilon x_1(T_0, T_1, T_2, \cdots) + \varepsilon^2 x_2(T_0, T_1, T_2, \cdots) + \cdots \tag{4}$$

By utilizing the condition for eliminating the secular terms that appear in the solution, the amplitude-frequency characteristic response can be determined. In engineering practice, the problems caused by the boundary disturbance of the lateral vibration of boring bars often possess symmetry. The main focus is on the positive boundary disturbance problem of the lateral vibration equation, and the width of the chip aw is much smaller than the feed amount and can be neglected. The lateral forced vibration equation of the boring bar - tool system.

$$\ddot{x} - c_{11}\dot{x} - c_{33}\dot{x}^3 + k_{11}x - k_{22}x^2 + k_{33}x^3 = \bar{F}\cos(\Omega t) \tag{5}$$

Based on the lateral vibration model of the BTA deep - hole boring bar, the first - order approximate solution of the system is obtained. It is advisable to use the multi - scale method to study the lateral vibration of the boring bar: $\Omega = \omega_0 + \varepsilon\sigma$ σ is the tuning parameter, and ε is an infinitesimal parameter. Introduce the time scales T_0=t, T_1=ε t; then the solution of the equation is: $x = x_0(T_0, T_1) + \varepsilon x_1(T_0, T_1)$, According to Eq (3):

$$\begin{cases} D_0^2 x_0 + k_{11}\omega_0^2 x_0 = 0 \\ D_0^2 x_1 + k_{11}\omega_0^2 x_1 = -2D_0 D_1 x_0 + \bar{c}_1 D_0 x_0 + \bar{c}_3 (D_0 x_0)^3 + \\ \bar{k}_2 x_0^2 - \bar{k}_3 x_0^3 + \varepsilon \bar{F}\cos(\omega_0 T_0 + \sigma T_1) \end{cases} \tag{6}$$

Let the solution of the first equation in Eq (6) be:

$$x_0 = A(T_1)\exp(i\omega_0 T_0) + \bar{A}(T_1)\exp(-i\omega_0 T_0) \tag{7}$$

It can be obtained from Eq (3) and Eq (7) :

$$\begin{cases} D_0 x_0 = i\omega_0 A\exp(i\omega_0 T_0) - i\omega_0 \bar{A}\exp(-i\omega_0 T_0) \\ D_0 D_1 x_0 = i\omega_0 \dot{A}\exp(i\omega_0 T_0) - i\omega_0 \dot{\bar{A}}\exp(-i\omega_0 T_0) \end{cases} \tag{8}$$

Using Euler's formula, the external force can be expressed in complex form as:

$$\cos(\omega_0 T_0 + \sigma T_1) = \frac{1}{2}\exp(i(\omega_0 + \sigma T_0)) + CC \tag{9}$$

Where $\bar{A}$ is the conjugate complex number of *A*, “CC” represents the complex conjugates of the preceding terms. *A*(T_1) is determined by the periodicity condition of *x*. Substituting Eq (8) and (9) into the second equation of Eq (6):

$$\begin{aligned} D_0^2 x_1 + k_{11}\omega_0^2 x_1 = (-2\dot{A} + c_{11}A + 3c_{33}A^2\bar{A})i\omega_0\exp(i\omega_0 T_0) - c_{33}Ai\omega_0\exp(3i\omega_0 T_0) + \\ A^2 k_{22}\exp(2i\omega_0 T_0) + A^3 k_{33}\exp(3i\omega_0 T_0) + 3A^2\bar{A}\exp(i\omega_0 T_0) + \\ \frac{1}{2}\bar{F}\exp(i(\omega_0 T_0 + \sigma T_1)) + CC + 2A\bar{A}\bar{k}_2 \end{aligned} \tag{10}$$

By eliminating the secular terms in Eq (10), we can obtain:

$$(-2\dot{A}+c_{11}A+3c_{33}A^2\overline{A})i\omega_0+\frac{1}{2}A^2k_{22}+\frac{3}{8}A^3k_{33}+\frac{1}{2}\overline{F}\exp(i\sigma T_1)=0 \tag{11}$$

In order to find A, express A as an exponential function.

$$A=\frac{1}{2}a\exp(i\beta) \tag{12}$$

It can be obtained from Eq (12).

$$\overline{A}=\frac{1}{2}a\exp(-i\beta)$$
$$\dot{A}=\frac{1}{2}\dot{a}\exp(i\beta)+\frac{1}{2}\beta a\exp(i\beta) \tag{13}$$

Substitute Eq (12) and (13) into Eq (11), and separate it into the real part and the imaginary part to obtain:

$$\begin{cases}\dot{a}=\frac{1}{2}c_{11}a+\frac{3}{8}c_{33}a^3+\frac{1}{2}\overline{F}\sin(\sigma T_1-\beta)\\ a\dot{\beta}=\frac{1}{2}a^2k_{22}+\frac{3}{8}a^3k_{33}-\frac{1}{2}\overline{F}\cos(\sigma T_1-\beta)\end{cases} \tag{14}$$

The first-order approximate solution is: $x=a\cos(t+\beta)+o(\varepsilon)$, let $\gamma=\sigma T_1-\beta$.

$$\begin{cases}\dot{a}=\frac{1}{2}c_{11}a+\frac{3}{8}c_{33}a^3+\frac{1}{2}\overline{F}\sin(\gamma)\\ a\dot{\gamma}=\sigma a-\frac{1}{2}a^2k_{22}-\frac{3}{8}a^3k_{33}+\frac{1}{2}\overline{F}\cos(\gamma)\end{cases} \tag{15}$$

When $\dot{a}=0$ and $\dot{\gamma}=0$:

$$\begin{cases}\frac{1}{2}c_{11}a+\frac{3}{8}c_{33}a^3+\frac{1}{2}\overline{F}\sin(\gamma)=0\\ \sigma a-\frac{1}{2}a^2k_{22}-\frac{3}{8}a^3k_{33}-\frac{1}{2}\overline{F}\cos(\gamma)=0\end{cases} \tag{16}$$

It can be obtained from Eq (16):

$$\begin{cases}(\frac{1}{2}c_{11}a+\frac{3}{8}c_{33}a^3)^2+(\sigma a-\frac{1}{2}a^2k_{22}-\frac{3}{8}a^3k_{33})^2=\frac{\overline{F}^2}{4}\\ \tan(\gamma)=-\dfrac{\frac{1}{2}c_{11}a+\frac{3}{8}c_{33}a^3}{\sigma a-\frac{1}{2}a^2k_{22}-\frac{3}{8}a^3k_{33}}\end{cases} \tag{17}$$

The above formula represents the amplitude - frequency response and phase frequency response obtained from the first order approximate solution of the system. By solving the lateral vibration equation of the BTA deep -hole boring bar-tool-cutting fluid system and the stability of the solution of the amplitude-frequency equation, numerical methods can be used to study the evolution trend of the system's nonlinear behavior. According to Lyapunov's first-order approximation theory, for the nonlinear system.

$$\frac{dx}{dt} = f(t,x) \tag{18}$$

If the Jacobian matrix of *f* with respect to *x* is:

$$\left.\frac{\partial f}{\partial x}\right|_{x=0} = A(t) \tag{19}$$

Then Eq (18) can be written as:

$$\frac{dx}{dt} = A(t)x + h(t,x) \tag{20}$$

When *h* (*t*, *x*) is an infinitesimal of higher order with respect to x in the neighborhood of *x*=0, the stability of Eq (15) can be studied by utilizing the stability of the linear system. To study the stability of the steady solution under the condition of the lateral vibration of the BTA deep - hole boring bar system, introduce the perturbation variable.

$$\begin{cases} a = a_0 - a_1 \\ \gamma = \gamma_0 - \gamma_1 \end{cases} \tag{21}$$

Where α_0, γ_0 is the steady solution of the steady-state motion, α_1, γ_1 is a small perturbation quantity. Substitute equation (21) into equation (15) , and perform a Taylor expansion on α_1 and γ_1, Considering that α_0 and γ_0 satisfy the following condition for Eq (15): Then, under the condition of retaining the linear terms, $\dot{a} + \dot{\gamma} = 0$ the approximate linear solution of the system regarding α1and γ1 can be derived.

$$\begin{cases} \dot{a}_1 = \frac{1}{2}c_{11}a_1 - \frac{9}{8}c_{33}a_0^2 a_1 + \frac{1}{2}\bar{F}\sin(\gamma)\gamma_1 \\ \dot{\gamma}_1 = a_1\frac{\sigma}{a_0} - a_0 a_1 k_{22} - \frac{9}{8}a_0^2 a_1 k_{33} - \frac{1}{2}\bar{F}\cos(\gamma)\gamma_1 \end{cases} \tag{22}$$

From Eq (15) and Eq (22), the characteristic equation can be obtained as follows:

$$diet\begin{bmatrix} \Phi_1 - \lambda & -\Phi_2 \\ \Phi_3 & \Phi_4 - \lambda \end{bmatrix} = 0 \tag{23}$$

Where:

$$\Phi_1 = \frac{1}{2}c_{11} - \frac{9}{8}c_{33}a_0^2; \quad \Phi_2 = a_0\sigma - k_{33}\frac{3}{8}a_0^3 - \frac{1}{2}a_0^2 k_{22}$$

$$\Phi_3 = \frac{1}{a_0}(\sigma - k_{33}\frac{9}{8}a_0^2 - \frac{1}{2}a_0 k_{22}); \quad \Phi_4 = \frac{1}{2}c_{11} + \frac{3}{8}c_{33}a_0^2$$

Expanding Eq (23), we can get:

$$\lambda^2 - (\Phi_1 + \Phi_4)\lambda + \Phi_1\Phi_4 + \Phi_2\Phi_3 = 0 \tag{24}$$

From this, the stability conditions for the steady solution of the system can be obtained as follows:

$$\begin{cases} \Phi_1 + \Phi_4 < 0 \\ \Phi_1\Phi_4 + \Phi_2\Phi_3 > 0 \end{cases} \tag{25}$$

The material of the BTA deep-hole boring bar is forged high-alloy structural steel. Analyze the stability of the lateral vibration of the BTA deep-hole boring bar - tool system under various parameters. When the external excitation frequency is close to the nonlinear frequency of the system, the violent vibration caused in the system is called the main resonance, and this vibration has a very significant impact on precision machining. Studying the influence of changes in system parameters on the main resonance has guiding significance for actual production.

3. Simulation analysis

3.1. Bifurcation analysis

By using the stability conditions of the steady-state solutions of the boring bar-tool system, the amplitude-frequency characteristics of the vibration equation are analyzed, and the influences of the technological parameters and the fluctuation of the force amplitude on the main resonance of the system are discussed. In Fig. 2, diagram (*a*) shows the variation diagram of the amplitude of the boring bar with the tuning value under the change of the primary damping coefficient c_{11}; diagram (b) shows the variation diagram of the main resonance of the boring bar with the primary damping coefficient c_{11} under different tuning values.

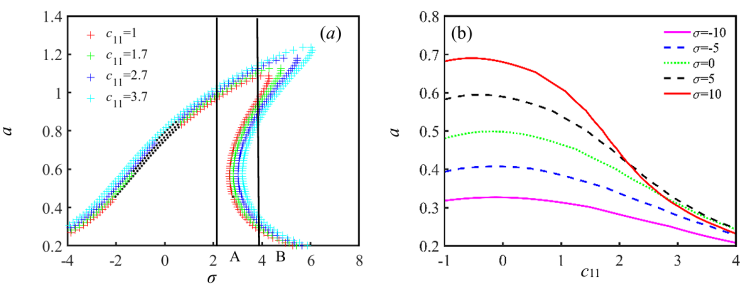

Figure 2. The amplitude-frequency characteristic diagram of the primary damping coefficient c_{11}

In Fig. 2(a), when the primary damping coefficient c_{11} is fixed, as the tuning value σ changes, the amplitude of the boring bar shows complexity. To the left of A, it increases monotonically, to the right of B, it decreases monotonically, and in the intermediate region, it exhibits complex nonlinearity, that is, both jumping and hysteresis coexist (in the interval [A, B] in Fig. (a)). When the tuning value σ is fixed, with the increase of the primary damping coefficient c_{11}, the lateral main resonance amplitude of the boring bar increases monotonically to the left of A and decreases monotonically to the right of B , and jumping and hysteresis occur in the interval [A, B]. It can be seen from Fig. 2(b) that the influence of the tuning value σ on the primary damping coefficient c11 presents obvious nonlinear characteristics, especially in the region near the right side of the value 0, this influence is particularly remarkable. When the system operates near the main resonance frequency, the parameter c_{11} should be controlled to avoid the jumping and hysteresis regions of the curve. According to formula (5), with the in-crease of the feed rate, the primary damping term gradually increases, and the uncertain interval of the system gradually expands. According to the analysis of formula (5) in section 2.3, the feed rates corresponding to the simulation values of the primary damping coefficient f in the curve of Fig. 2 are 0.91 mm/s, 2.47 mm/s, 4.68 mm/s, and 6.89 mm/s, indicating that the more the feed rate increases, the more obvious the nonlinear behavior of the system is.

In Fig. 2, diagram (a) is a graph of the change of the lateral main resonance amplitude of the boring bar with the tuning value under different cubic damping coefficients c_{33}; diagram (b) is a graph of the change of the lateral main resonance of the boring bar with the cubic damping c_{33} under different tuning values.

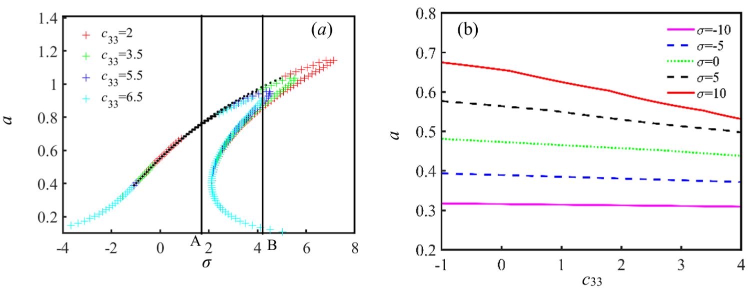

Figure 3. The amplitude-frequency characteristic diagram of the cubic damping coefficient c_{33}

It can be concluded from Fig. 3(a) that when the tuning value σ is fixed, with the increase of c_{33}, the change of the resonance amplitude is monotonically increasing jumping and hysteresis - monotonically decreasing. The peak position of the amplitude-frequency response curve remains stable and does not shift with the change of system parameters. This phenomenon reveals that the cubic damping coefficient mainly regulates the vibration intensity of the combined resonance and has no significant effect on the tuning frequency of the main resonance. It can be seen from Fig. 3(b) that under the condition of a given tuning value σ, with the increase of the cubic damping coefficient c_{33}, when the system parameters are in the region to the left of point A, the vibration amplitude shows an approximately linear growth trend.

In Fig. 4, diagram (a) is a graph of the change of the lateral main resonance amplitude of the boring bar with the tuning value when the quadratic stiffness coefficient k_{22} changes; diagram (b) is a graph of the change of the lateral main resonance of the boring bar with the quadratic stiffness coefficient k_{22} under different tuning values.

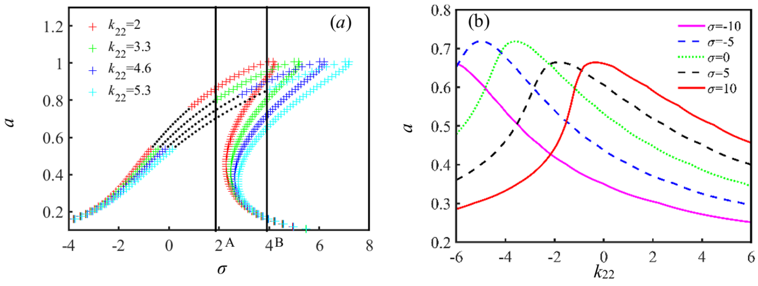

Figure 4. The amplitude-frequency characteristic diagram of the quadratic stiffness coefficient k_{22}

It can be known from Fig. 4(a) that when the quadratic stiffness coefficient is fixed, with the increase of the tuning value, the amplitude of the system response shows typical nonlinear evolution characteristics: in the initial stage, it shows a linear growth trend, and then the dynamic behavior changes abruptly, and the amplitude jumping phenomenon occurs, accompanied by an obvious hysteresis effect. Under the condition of a given tuning value σ, with the increase of the quadratic stiffness coefficient k_{22}, the amplitude region of the lateral main resonance of the boring bar increases (the interval [A, B] in the figure). The tuning value σ has different influences on the quadratic stiffness coefficient k_{22}. The tuning values greater than around 2 have a greater influence on the quadratic stiffness coefficient k_{22}, showing nonlinear behavior.

It can be seen from the analysis of formula (5) that the change of the quadratic stiffness term is affected by the elastic deformation of the tool. The greater the elastic deformation of the tool caused by cutting, the more the chips accumulate on the rake face of the tool, and the greater the quadratic stiffness coefficient. With the increase of the quadratic stiffness coefficient, the multi-valued jumping interval increases significantly. The selection of the tool mate-rial will also affect the state and degree of elastic deformation of the tool during the working process. The elastic deformation of the tool during the cutting process will cause significant nonlinear instability of the boring bar. It is verified from Fig. 4(a) that the selection of the tool material has a certain influence on the stability of the machining system. With the force on the tool material during the machining process and the increase of elastic deformation, the multi-valued jumping phenomenon of the system solution will occur. With the increase of the cutting speed, the built-up edge gradually decreases when reaching medium and high-speed cutting, resulting in a decrease in the quadratic stiffness coefficient. It can be known from Fig. 4(b) that when the value of the stiffness coefficient k_{22} is fixed, with the increase of the tuning value σ, the change of the vibration amplitude shows complex nonlinearity. From the analysis of the quadratic stiffness coefficient k_{22}, the cutting speed affects the notch pressure, and then affects the value of the parameter k_{22}. It can be seen from Fig. 4(b) that the larger the k_{22}, the smaller the amplitude, indicating that high-speed cutting can avoid system instability and thus improve the machining quality of the workpiece, which is consistent with the previous conclusion. However, the nonlinear behavior at medium and high cutting speeds is complex, and the specific internal mechanism and influence law are mainly studied through the bifurcation analysis of the specific motion law under the change of parameters.

In Fig. 5, diagram (*a*) is a graph of the change of the main resonance of the boring bar with the tuning value under the change of different cubic stiffness coefficients k_{33}; diagram (b) is a graph of the change of the main resonance of the boring bar with the cubic stiffness coefficient k_{33} under different tuning values.

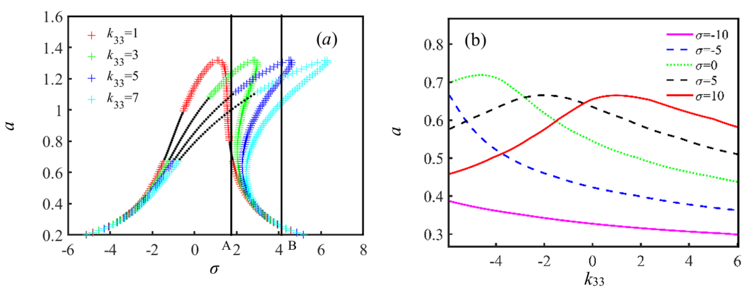

Figure 5. The amplitude-frequency characteristic diagram of the cubic stiffness coefficient k_{33}

It can be seen from Fig. 5(a) that when k_{33} is constant, with the increase of σ, the vibration amplitude shows complex nonlinear phenomena in the interval [A, B]; when σ is constant, with the increase of the value of k_{33}, the vibration amplitude decreases, and the vibration amplitude region shows complex behavior within the interval [A, B], but shows monotonicity outside the interval. It can be known from Fig. 5(b) that there is a significant nonlinear coupling relationship between the system tuning parameter σ and the cubic stiffness coefficient k33. When the tuning value is in the positive interval (σ > 0), the response sensitivity of the system to the change of the k_{33} parameter is significantly enhanced, and this parameter sensitivity presents an asymmetric distribution characteristic with the change of the tuning value. When the value of σ is constant, with the increase of k_{33}, the behavior of the system vibration amplitude is complex. When $\sigma < 5$, the system vibration amplitude first increases linearly and then decreases linearly. When $\sigma > 5$, the system vibration amplitude decreases linearly; when k_{33} is on the left side of 0, with the increase of σ, the vibration shows overlapping jumps; when k_{33} is on the right side of 0, with the increase of σ, the vibration shows a mono-tonic decrease.

In Fig. 6, diagram (*a*) is a graph of the change of the lateral main resonance amplitude of the boring bar with the tuning value under different external force values *F*; diagram (b) is a graph of the change of the lateral main resonance of the boring bar with the force amplitude value *F* under different tuning values.

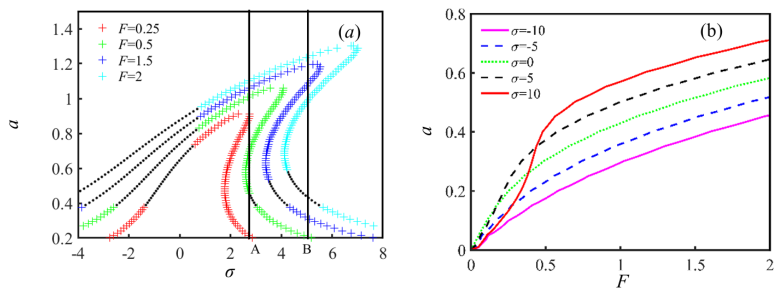

Figure 6. The amplitude-frequency characteristic diagram of the force amplitude value *F*

It can be seen from Fig. 6(*a*) that when *F* is constant, with the increase of σ, the vibration amplitude of the system changes from monotonically increasing to jumping and hysteresis, showing typical nonlinearity; when σ is constant, with the increase of the external excitation amplitude F, both the lateral main resonance amplitude of the boring bar and the nonlinear interval of the main resonance increase. The flow state of the cutting fluid will affect the magnitude of the force amplitude. When the flow rate of the internal cutting fluid is large, the force amplitude is large, and the nonlinear characteristics of the motion system of the boring bar are remarkable and the multi-valued jumping interval increases. It can be known from Fig. 6(b) that when F is constant, when the dimensionless force amplitude F is on the left side of 0.5, with the increase of σ, the vibration shows overlapping jumps; when the dimensionless force amplitude *F* is on the right side of 0.5, with the increase of σ, the vibration shows a monotonic increase. When the dimensionless force amplitude is on the left side of 0.5 and the feed rate is 4.26 mm/s at this time, the uncertainty of the system amplitude will cause the in-stability of the system, which is caused by the weak anti-interference ability of the boring bar system to the sudden force. The quadratic stiffness coefficient of the system changes abruptly from 0, causing the chips to accumulate on the rake face, and the actual working angle of the tool changes, resulting in the uncertainty of the system amplitude.

4. Conclusions

Based on the above analysis of the amplitude frequency characteristics, it can be known that the changes in the dimensionless primary damping coefficient and the force amplitude depend to a certain extent on the change in the feed rate. The change in the dimensionless primary damping coefficient will trigger the nonlinear behavior of the boring bar - tool system. According to the analysis results of the amplitude - frequency characteristics of the dimension-less primary damping coefficient, when the system feed rate is greater than 6.29 mm/s, the system exhibits nonlinear characteristics. The change in the force amplitude is mainly caused by the influence of the feed rate and the cutting fluid. From the amplitude - frequency characteristic diagram, it can be obtained that the change in the state and flow rate of the cutting flu-id affects the force amplitude. When the feed rate is less than 4.26 mm/s, it will cause an un-certain state of the system. From the analysis of the amplitude frequency characteristic parameters of the dimensionless secondary stiffness, it can be seen that an increase in the elastic deformation of the tool under force will lead to an increase in the amplitude of the nonlinear vibration of the system, and the nonlinear region of the system vibration equation will gradually increase. The underlying reason for this change is caused by the increase in the cutting depth. The main cause of the influence of the change in the force amplitude on the vibration behavior of the boring bar is the change in the cutting force. An increase in the disturbing force will make the nonlinear characteristics of the boring bar vibration more significant.

References

[1] Li L, Ren Y, Shen Z, et al. Nonlinear system optimization of cutting tools with dynamic vibration absorbers in deep hole boring: A stability analysis[J]. Alexan-dria Engineering Journal, 2025, 112: 246-253.

[2] Donghui Y, Yongsheng R, Yuhuan Z, et al. Nonlinear dynamics of cutting pro-cess considering higher-order deformation of composite cutting tool[J]. Shock and Vibration, 2021, 2021: 1-12.

[3] Ma B, Ren Y. Nonlinear dynamic analysis of the cutting process of a nonex-tensible composite boring bar[J]. Shock and Vibration, 2020, 2020: 1-12.

[4] Xiaokang D, Jing Z, Xian G, et al. Dynamics analysis of rotating cantilever beams with free end mass[J]. Applied Sciences, 2022, 12(15): 7553.

[5] Weitao D, Liming W, Dingqiang P, et al. A new dynamic boring force calcula-tion method using the analytical model of time-varying toolpath and chip frac-ture[J]. Journal of Materi-als Processing Technology, 2022, 306: 1-12.

[6] Lu K, Gu F, Longstaff A, et al. An investigation into tool dynamics adaptation for chatter stability enhancement in the turning of flexible workpieces[J]. The In-ternational Journal of Advanced Manufacturing Technology, 2020, 111(11-12): 1-13.

[7] Zhang C, Ren Y, Ji S, et al. Analysis of the composite boring bar dynamic char-acteristics considering shear deformation and rotational inertia[J]. Applied Sci-ences, 2020, 10(4): 1-15.

[8] Yao Q, Luo M, Zhang D, et al. Identification of cutting force coefficients in ma-chining process considering cutter vibration[J]. Mechanical Systems and Signal Processing, 2018, 103: 39-59.

[9] Chen X, Wang Q, Chen W, et al. Mining method for cutting force coefficient with the

im-pact of tool vibration and machine tool system[J]. Advances in Me-chanical Engi-neering, 2024, 16(12): 1-12.

[10] Al-Wedyan H M, Hayajnem M T. Dynamic modelling and analysis of whirling motion in BTA deep hole boring process[J]. International Journal of Ma-chining & Machinability of Materials, 2011, 10(1/2): 48-70.

[11] Weinert K, Webber O, Peters C. On the influence of drilling depth de-pendent modal damping on chatter vibration in BTA deep hole drilling[J]. CIRP Annals-Manufacturing Technology, 2005, 54(1): 363-366.

[12] Perng, Nayfeh A H. A nonlinear composite beam theory[J]. Nonlinear Dynamics, 1992, 3(4): 273-303.

[13] Quanbin Z, Wu Z, Yamin L. Transverse vibration of the boring bar for BTA deep hole machining under stochastic excitation[J]. Journal of Mechanical Science and Technology, 2023, 37(11): 5635-5648.

[14] Ma G, Shen X. Eigensolution of a BTA deep-hole drilling shaft system[J]. Journal of Me-chanical Science and Technology, 2018, 32(4): 1499-1504.

[15] Quanbin Z, Wu Z, Yamin L, et al. Transverse vibration of the boring bar for BTA deep hole machining under stochastic excitation[J]. Journal of Mechanical Science and Tech-nology, 2023, 37(11): 5635-5648.